Benha Journal of Applied Sciences (BJAS) print: ISSN 2356–9751
Vol. (9) Issue (3) (2024), (207-217) online: ISSN 2356–976x
http://bjas.bu.edu.eg

Structural mapping and kinematic history of the Qena-Safaga Shear Zone (Egyptian Nubian Shield, East African Orogen)

Asmaa.E.El-Araby[1*],Wael.D. Hagag[1], Samir.Z.Kamh[2] and Zakaria.E.Hamimi[1]
[1] Geology Department, Faculty of Science, Benha University, Benha 13518, Egypt
[2] Geology Department, Faculty of Science, Tanta University, Tanta 31527, Egypt
E-Mail: asmaageol@gmail.com

Abstract

The Qena- Safaga Shear Zone (QSSZ) is a megashear belt separating the Northern- and the Central- Tectonic Provinces of the Egyptian Nubian Shield (ENS). Processing of remotely sensed data of the Landsat-8, ASTER and Sentinel 2A, accompanied by field/structural investigation made it possible to construct a plausible structural map for this high strain zone. A wide variety of Neoproterozoic litho-units outcrop in the area, including ophiolitic mélange, syn- tectonic granitoids, late- tectonic granitoids, Dokhan Volcanics and post- tectonic granitoids. Dike swarms traverse some of these units. The automatic lineament extraction using SRTM and PALSAR images verified that the dominant structural trend is the NE-SW. Other trends, comprising E-W (to ENE-WSW), NW-SE (to NNW-SSE) and N-S (to NNE-SSW) are also recognized. The main structural elements documented in the area embrace foliations and lineations, faults and shear zones, as well as shear zone-related structures (e.g. folds, duplexes and flower structures). The sense of movement along the aforementioned shear trends can be detected by a wide variety of kinematic indicators include mylonite, boudinage structure and deformed pebbles. The geological structures documented along the QSSZ indicate a brittle-ductile tectonic regime accompanied with voluminous granitic intrusions of various composition. Such structural and tectonic setting advocates a complex tectonic history characterized by extensional and transtensional tectonic regimes. The obtained results are significantly contributed to our knowledge on the high strain shear belts in the ENS.

Keywords: Qena- Safaga Shear Zone, SRTM/PALSAR data, Shear zone-related structures, Dokhan Volcanics.

1. Introduction

The Qena- Safaga Shear Zone (QSSZ) is one of the shear belts in the Egyptian Nubian Shield (ENS). It separates the Egyptian Northern and Central Eastern Deserts [1-3].Several issues need to be addressed concerning the QSSZ including the sense, time and scale of shearing, as well as its relation to the Najd Fault System (NFS). The structural setting and tectonic evolution of the QSSZ is a matter of debate according to the nature of shear sense that is initiated as dextral then reactivated as sinistral in post-Miocene time [4]. The study area is located at the boundary between the NED and CED (Fig.1), and delineated by latitudes 26° 20´ to 26° 30´N and longitudes 33° 10´ to 33° 34´E. It occupies the central part of the Qena –Safaga asphaltic road, which makes the area more accessible for geological investigation. Numerous mountain peaks are exposed in the study area, such as El Dob, El-Urf, Abu Shihat, Kafari, Semna, Rie-el-Garra, El-Missikat, El- Erediya, El Maghrabiya and Kab Amiri (Fig.2). Moreover, the study area has an economic importance, especially for the prospecting and exploration of gold, REEs and radio-elements [5].Many petrological, geochemical and structural studies have been conducted for the study area [6-18].

The main objectives of the present study are: (1) utilizing of remote sensing data (Landsat-8, ASTER and Sentinel 2A) and field-structural study in geological and structural mapping of the study area, (2) deciphering the structural setting and tectonic evolution of the study area, and (3) using the lineament extraction method in evaluating the lineaments and determining the dominant structural trends deforming the Neoproterozoic basement rocks outcropping at the study area.

2. Methodology

2.1. Methodology of lithological mapping

The present study depends essentially on the processing and analysis of remotely sensing data and field-structural study. High resolution mapping of the different basement rock units using the pre-processing and processing of the Landsat-8, ASTER and Sentinel 2A images resulted in a prominent classification of the basement succession of the area into ophiolitic mélange, syn–tectonic granitoids, late–tectonic granitoids, Dokhan Volcanics and post-tectonic granitoids (Fig.3). The remote sensing techniques used in lithological mapping and rock unit include False Color Composite, Principal Component Analysis, Band Ratioing and Mineral Indices.

2.2.Methodology of lineaments analysis

In the present study, images used in lineaments extraction include the Advanced Land Observing Satellite (ALOS), the Phased Array type L-band Synthetic Aperture Radar (PALSAR with resolution of 12.4 m), Digital Elevation Model (DEM) of Shuttle Radar Topography Mission (SRTM), and hill shaded or shaded relief images extracted from the DEM image with 30 m resolution. The PCI Geomatica 2018, Pock Work Steronet, Surfer and Global Mapper Software have been used for lineament extraction. The algorithm of PCI Geomatica software includes edge detection, thresholding and curve extraction steps (PCI Geomatica, 2018). The parameters applied for the lineament extraction by the LINE Module are shown in Table (1).

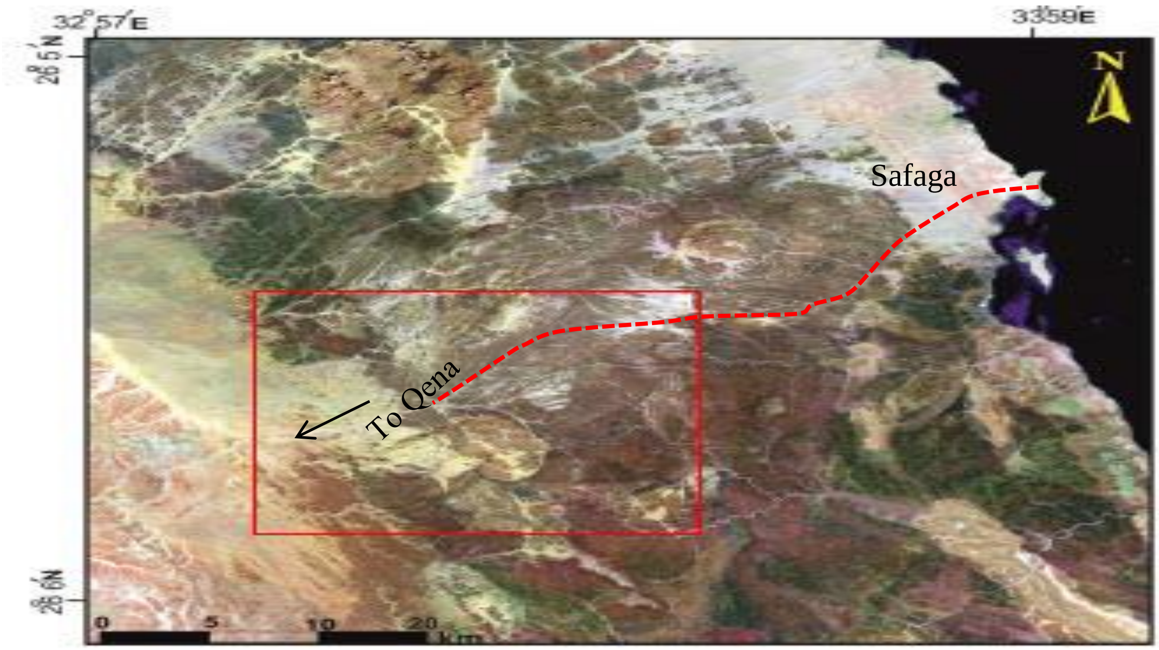

Fig (1) Sentinel 2 A satellite image with 10m resolution whereas the study area is cleared by red rectangle and the Qena-Safaga road by red dashed line.

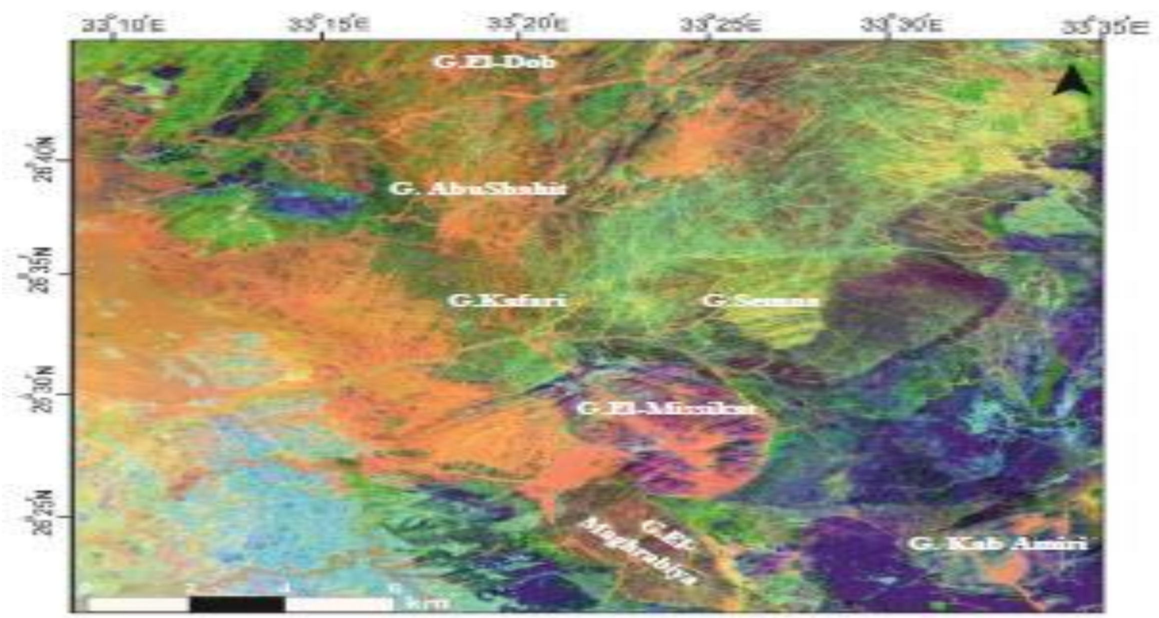

Fig (2) Band ratio combination RGB(4/3, 6/7, 6/5) of landsat-8 discriminate the different mountains in the study area including G. El-Dob, G. AbuShahit, G.Kafari, G. El-Missikat, G.Rie El- Garra, G.El- Maghrabiya G.EL- Eridiya and G. Kab Amiri) in different color.

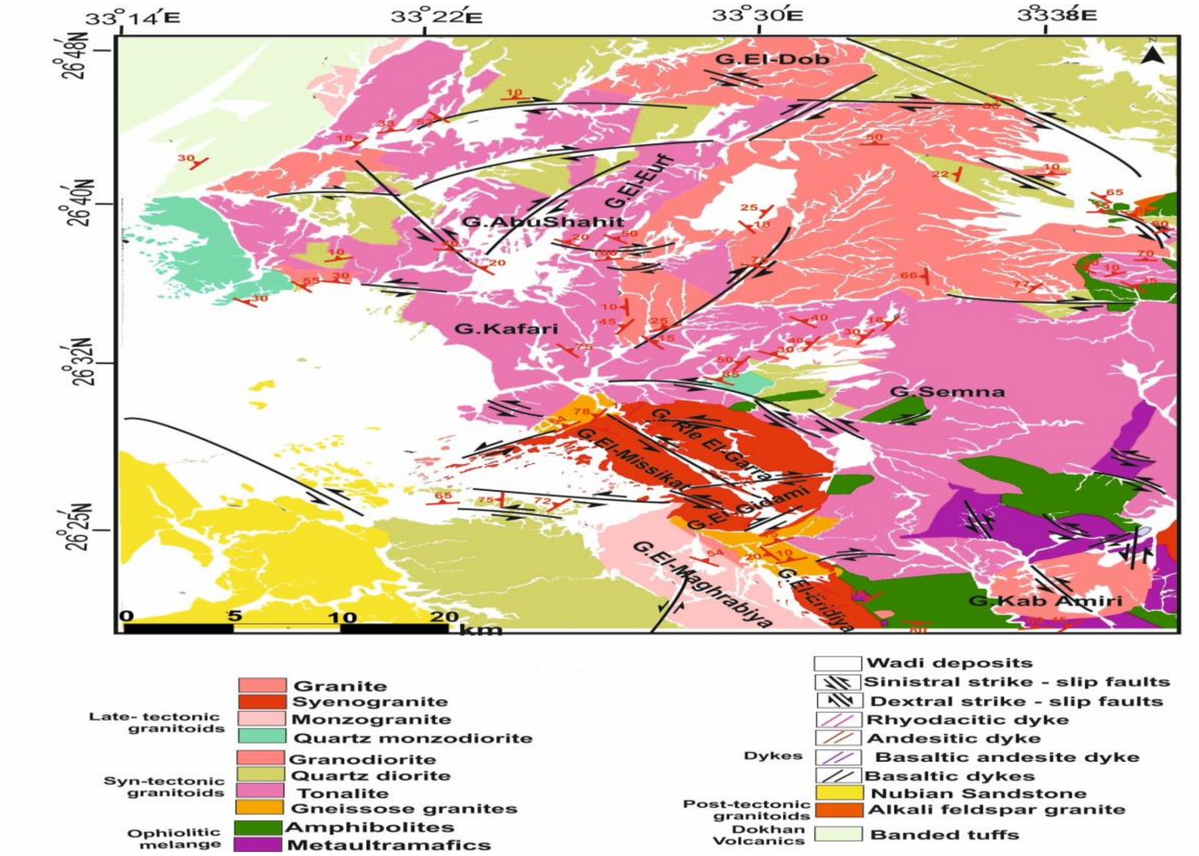

Fig (3) Geologic map of the study area (constructed based on image processing of Landsat-8, ASTER, Sentinel2 A data, besides the field/structural work and ground truth).

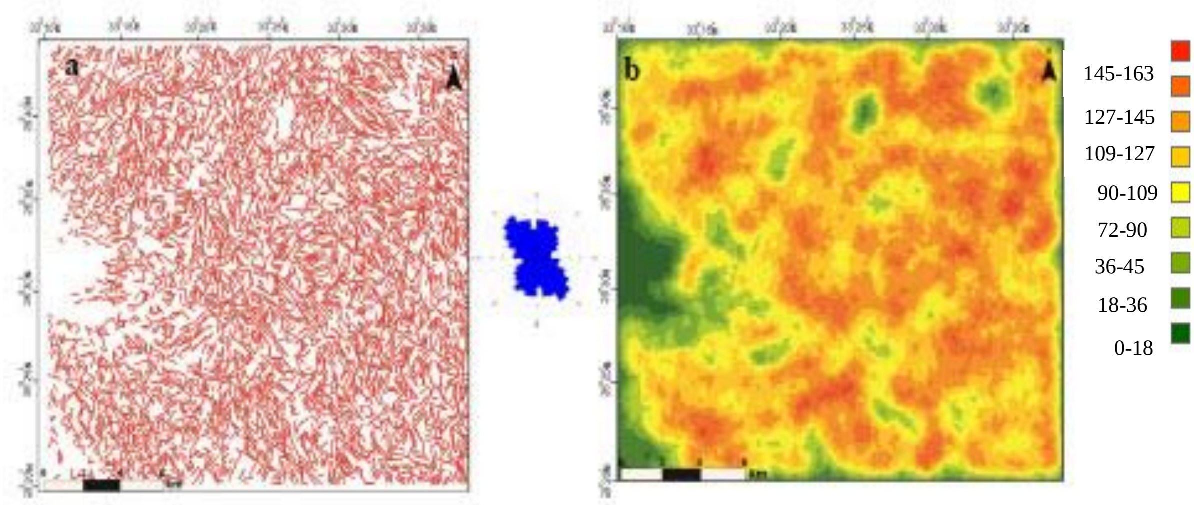

Fig (4)(a).Lineaments map extracted from PALSAR data (b) Lineaments density map of PC1 of combined HH+HVof PALSAR concentrated in the northern part of the study area and showing NW and NE trends.

Table (1) Parameters used for the PCI Geomatica software (after [25]).

Name	Description	Values (Pixels)
RADI	Radius of filter in pixels	10
GTHR	Threshold for edge gradient	20
LTHR	Threshold for curve length	20
FTHR	Threshold for fitting error	7
ATHR	Threshold for angular difference	15
DTHR	Threshold for linking distance	20

2.2.1. Results of lineament extraction

Automatic lineaments extraction based on the PALSAR data

The lineaments can be extracted manually or automatically [19-24]. In this study, lineaments were extracted automatically from the PALSAR data by using the PCI Geomatica version 2018. The automatic lineaments were extracted from the PC1 by combining the HH (Horizontal-Horizontal) and the HV (Horizontal-extracted, ranging in size from 600m to 3848 m with total length reaching 3363m. These lineaments are longer in NW-SE and NE-SW, while shorter in N-S and E-W directions, respectively (Fig.4a).

The different trends are confirmed by the density map (Fig.4b). The moderate density lineaments exhibit yellow Vertical) and HH+HV images of PALSAR. Some 3132 lineaments have been color and the low density lineaments appear in green color in the western part. The latter affect the Nubian Sandstone and reflect little effect of tectonism in contrast to the lineaments that appear with high concentration (red) and associating with the granitic plutons and alteration zones.

Extraction of lineaments from the shaded relief image

Lineaments can be extracted from the shaded relief images produced from DEM. This method depends on the illumination of the lineaments achieving at different orientations by assuming topographic illumination under varied light directions. Four shaded relief images were used to identify and detect the linear topographic features from the DEM. Firstly, the production of shaded relief images achieved through light sources (solar azimuth) coming from different directions [26]. In the present study, four different directions 0˚, 45˚, 90˚, 135˚ have been applied.

In the case of 0˚, the number of lineaments is 367 with total length reaches up to 13761m. The longest lineaments follow the ENE-WSW and WNW-ESE directions, while the lineaments in the NE-SW and NW-SE trends are the shortest (Fig.5a). Most lineaments with low density reflect green color, while lineaments with high density appear in the northern part of the study area especially in Gabals El-Eurf and Abu Shahit (Fig. 5b).

In the case of 45˚, the number of lineaments is 349 with total length reaches to about 13866 and the main trend of theselineaments is NE-SW (Fig. 5c). These lineaments display high concentration (red color) all over the area except in the western part which is characterized by low density (Fig. 5d). In the case of 90˚, lineaments with NNW-SSE and NNE-SSW trends (Fig.6a) are concentrated in the northern and southern parts of the study area without any concentration in the central part (Fig. 6b). In the case of 135˚, the lineaments are about 322, with total length reaching about 12109 m, where the longest lineaments follow the NW-SE trend (Fig. 6c) and the density map showing high concentration of lineaments in the NW-SE trend (Fig.6d).

By applying the different parameters of PCI Geomatica on the image extracted from the combination of four shaded relief images (0˚, 45˚, 90˚, 135˚), the lineaments extracted are 183 with total length reaching up to 6397 m and with NNE to NE as the main trend, and the N-S as an auxiliary trend (Fig.7a). The lineaments with high density are concentrated in the northern part of the area compared to the southern part in which the lineaments of low density do exist (Fig.7b).

3. Structural setting and tectonic evolution

3.1. Structural setting

The QSSZ is one of the eye-catching structural elements in the ENS. It was ragarded as the tectonic boundary between the NED and the CED. Detailed field investigation indicates that the QSSZ- related geological structures range from submicroscopic- scale up to regional-scale. As the granitic plutons of various types are the dominant lithological units in the study area, the most affecting tectonic structures are brittle-ductile fractures such as faults, joints, shear zones and related structures. Figure (8) shows the structural map of the study area that is constructed based on the integrated remote sensing data analysis and the field study.

3.1.1.Shear zones and faults

Shear zones are one of the most remarkable structures deforming the rock units in the study area. The structural trends of these zones include E-W (to ENE-WSW), NW-SE and N-S (to NNE-SSW and NNW-SSE), besides the NE-SW trend (see Fig. 8).

E-W to ENE –WSW shear trends

The E-W to ENE-WSW shears are the oldest trends recorded in the study area. The sense of movement along these trends is dextral. The E-W shear trend is common and has recorded in the gneissose granite located in the northwestern part of the study area and also south of El-Missikat pluton. It is also recorded in El-Maghrabiya pluton where it is traversed by the NW-SE shear trend (Fig.9a).

N-S, NNW-SSE, NW-SE and WNW- ESE shear trends

The sinistral N-S shear trend traverse gneissose granite located to the south of El-Missikat pluton (Fig. 9b). The Quartz diorite located west to Gabal Rie El-Garra is sheared in the NNW-SSE trend (Fig. 9c). The NW-SE shearing is common in the study area with sinistral sense of shearing. NW trend (N30°W) is common in the syenogranite of Rie El-Garra pluton (Fig. 9d).

NE-SW and NNE-SSW shear trends

The NE-SW and NNE-SSW shears are the youngest trends in the study area. The sense of movement along these shears is dextral. This trend is recorded in the quartz diorite located north of Gabal Semna (Fig10a). The NE shear trend dissects the NW-SE shearing trend in Rie El-Garra syenogranite (Fig.10b).

3.1.2. Shear zone-related structures

Duplex structure

Duplex structures are associated with the NE-SW to ENE-WSW shearing and propagated toward the ESE direction (S80°E). These structures are observed in Rie El-Garra syenogranite (Fig10c).

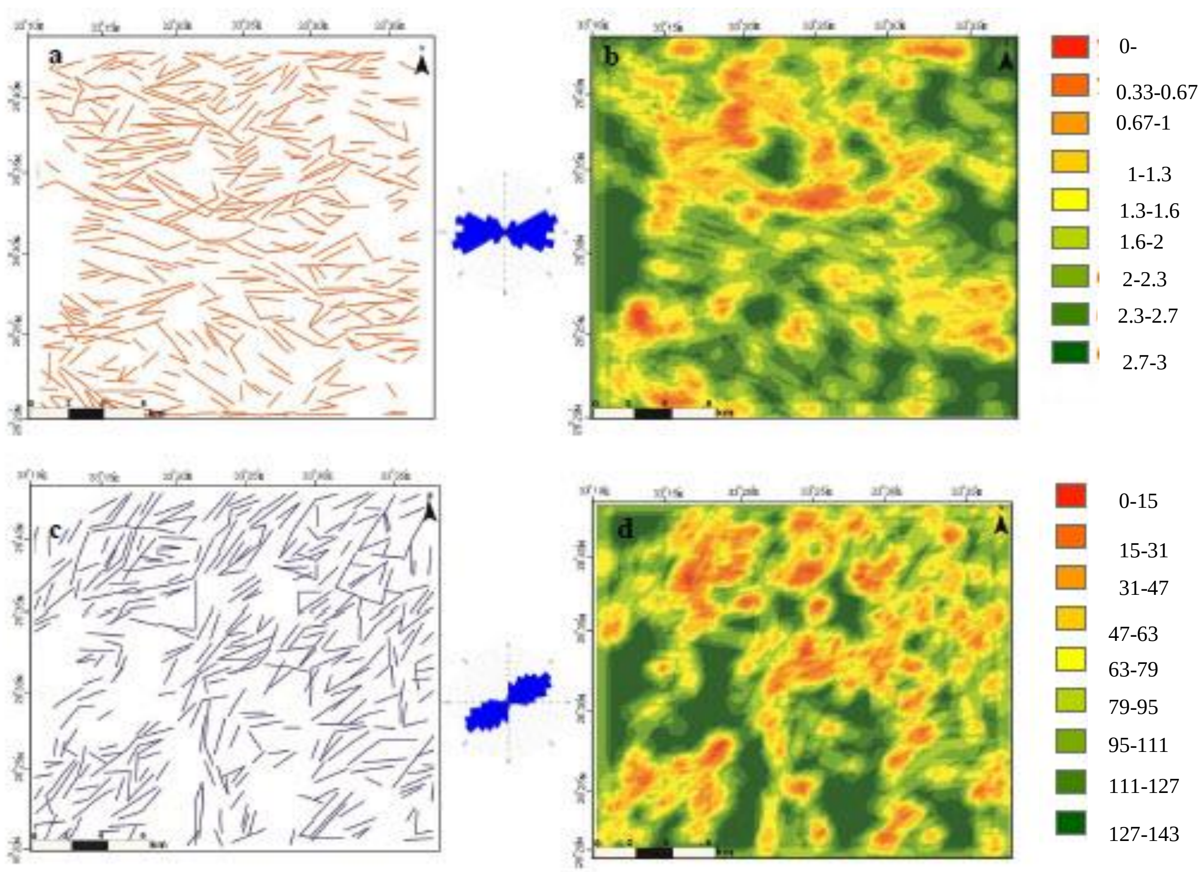

Fig(5) (a) Lineaments map extracted from the shaded relief image with sun angle azimuth (0˚) and rose diagram showing the ENE- WSW and WNW-ESE trends. (b). Lineaments density map extracted from the shaded relief image of sun azimuth (0°) and lineaments concentrated mainly in the northern part of the study area and showing the EW trend. (c)Lineaments density map extracted from the shaded relief image of sun azimuth (45°) and lineaments concentrated mainly in the northern part of the study area and and rose diagram showing the NE-SW as the main trend. (d) Lineaments density map extracted from the shaded relief image of sun azimuth (45°) showing the NE-SW and E-W trends.

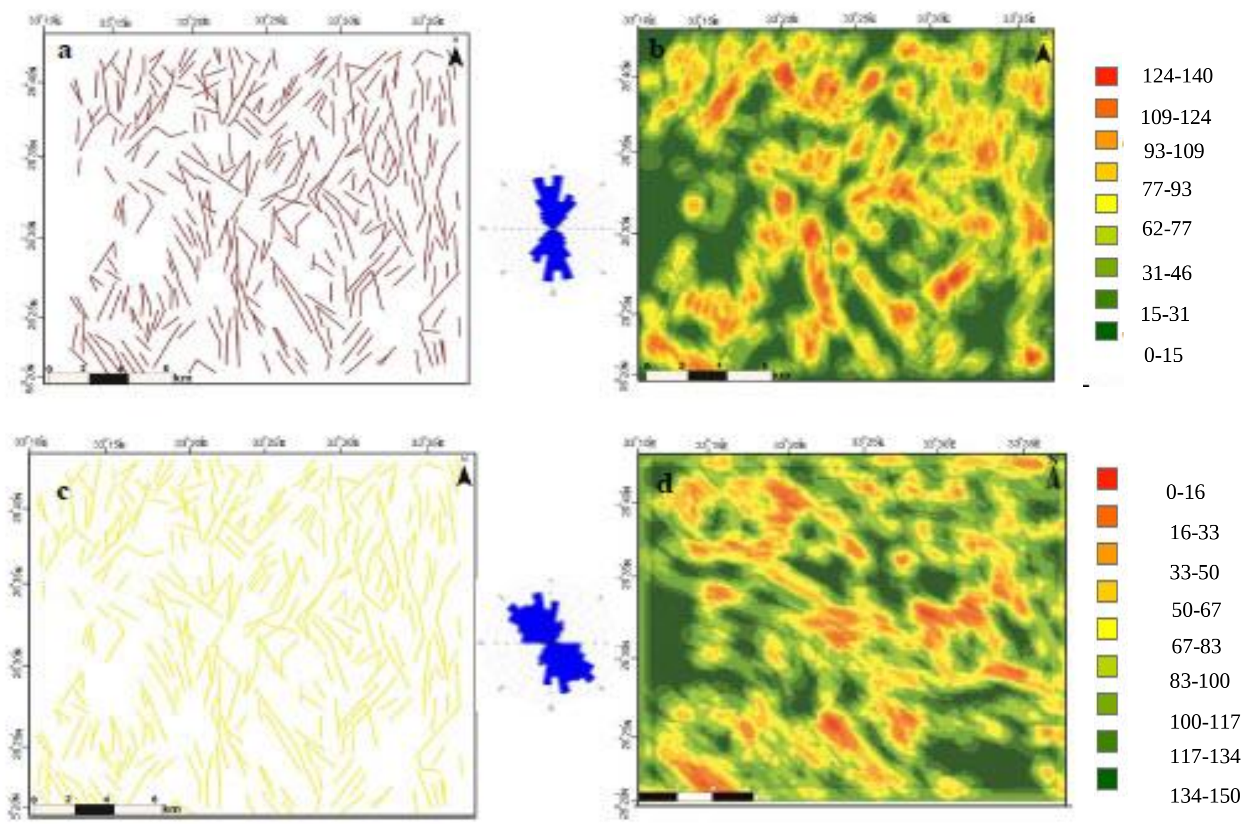

Fig (6)(a) Lineaments map extracted from the shaded relief image with sun angle azimuth (90˚) and rose diagram showing the NNE-SSW and NNW-SSE trends. (b) Lineaments density map extracted from the shaded relief image of sun azimuth (90°) showing that lineaments with NNE-SSW and NNW-SSE trends. (c) Lineaments map extracted from the shaded relief image with sun angle azimuth (134˚) and rose diagram showing the NW-SE trend with NE and N-S trends. 3(d) Lineaments density map extracted from the shaded relief image of sun azimuth (134°) showing NW-SE is the main trend.

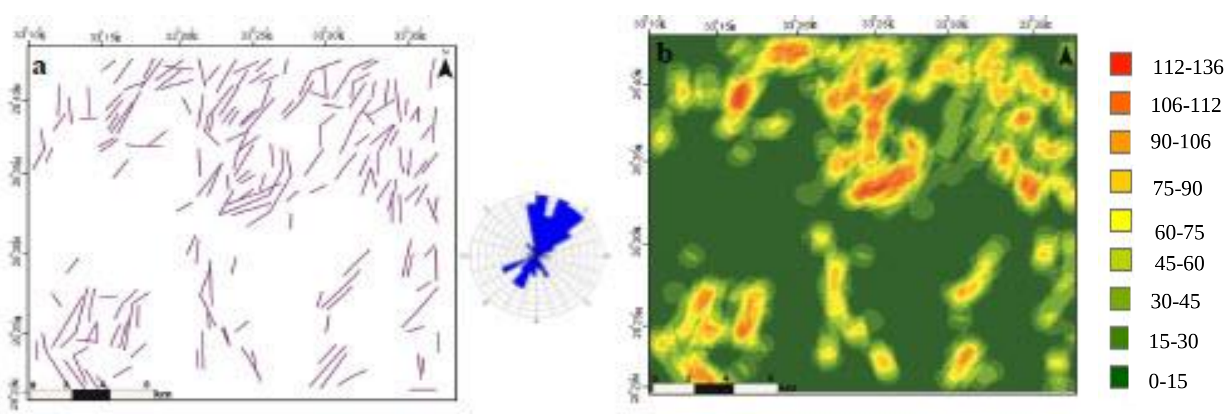

Fig(7)(a). Lineaments map extracted from the shaded relief image produced from the combination of four sun azimuth angles 0˚ , 45˚ , 90˚ , 135˚ and rose diagram showing the NNE to NE trend. (b) Lineaments density map extracted from the four shaded relief image with different sun azimuth angles including (0˚, 45˚, 90˚, 135˚) showing that lineaments are concentrated in the northern part compared to the southern part of the study area with NNE to NE trends.

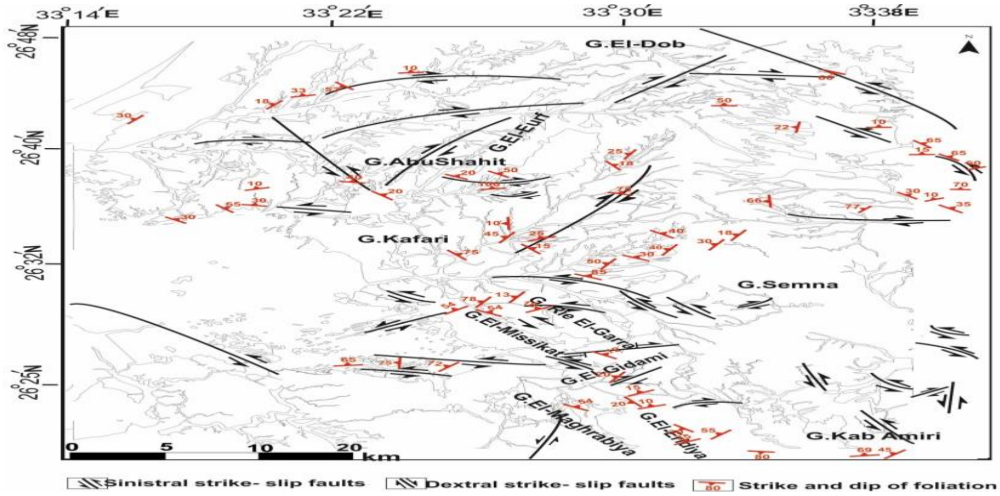

Fig (8) Structural map of the study area.

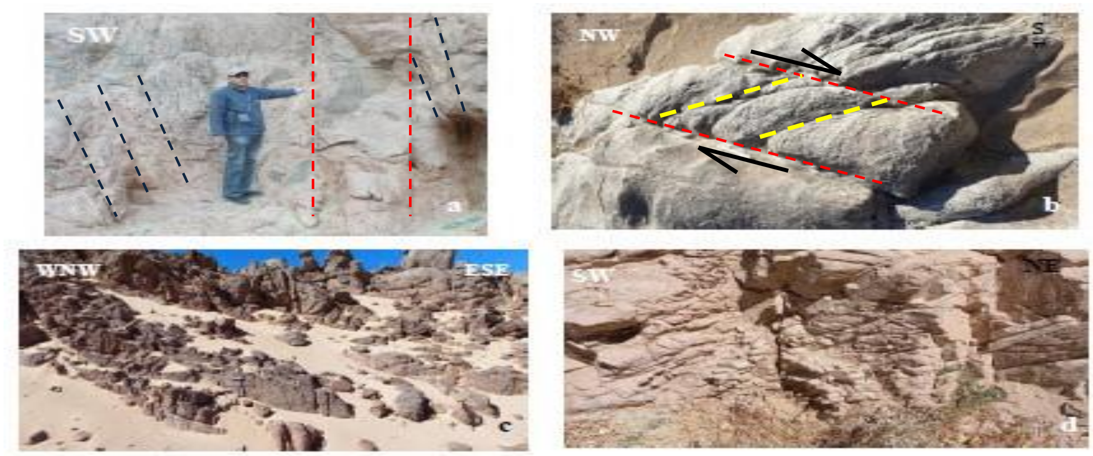

Fig (9) (a) E-W trending quartz veins dissecting El-Maghrabiya monzogranite (b) N-S shear trend in the gneissose granite located to the south of El-Missikat pluton (c) NW-SE shearing in the quartz diorite located west to G.abal Rie El-Garra (d) NW-SE shearing in the Rie El-Garra syenogranite.

Fig (10) (a) NW-SE shearing in the quartz diorite located west to G.abal Rie El-Garra (b) NS shearing trend dissected by the NE-SW trend in the tonalitic rocks of Semna pluton . (c) Thrust duplex structure in Rie El-Garra syenogranites associating with the NE-SW to ENE-WSW shearing (d) Flower structure accompanying with the E-W shearing in the gneissose granite located at north western part of Rie El-Garra pluton.

Flower structure

Flower structures are detected in the gneissose granite that is located at the northwestern part of Rie El-Garra pluton and associated with E-W shear trend (Fig.10d).

Shear Zone-related folds

Shear zone=related folding, which is also referred to as slip folding, involves shearing along planes that are oriented approximately parallel to the axial plane of the fold structure. In the study area, such folds are recorded in El-Gidami syenogranite, associated with the NE-SW shearing (Fig.11a). They are also recorded in the Dokhan Volcanics accompanying with ENE-WSW trending (Fig.11b)

3.1.3. lineations and foliations

A lineation is a term used to describe any fabric element represented by a line where one dimension is longer than the other [27]. The following types of lineations are documented from the study area.

Stretched lineation

Stretched lineation is a general term used for aggregate lineation or grain lineation if the constituting grains are defined by deformed aggregates or single crystal .In the concerned area, stretched lineation exist as stretched xenoliths of amphibolite rocks in El-Kafari tonalite (Fig.11c).

Mineral lineation

Mineral lineation forms when a single or sets of minerals arranged on the surface of a surface of quartz diorite rocks located west of El- Maghrabiya pluton accompanying the E-W shearing (Fig.11d).

Pencil-like lineation

Pencil lineation formed as a result of interference between compaction cleavage and a subsequent cleavage or between two equally developed tectonic cleavages taking a preferred orientation [28].In the study area, this lineation is recorded in metaultramafic rocks located to the south of Kab Amiri pluton in association with the ENE- WSW and NW- SE shear trends (Fig. 12a).

Foliations refer to any planar fabric types in rocks [27].Different types of foliations are recorded in the area, such as gneissic foliation in the gneissose granite outcropping at the northern part of Rie El-Garra pluton (Fig.12b), and the mylonitization foliation recorded in the syenogranites of El-Missikat pluton (Fig.12c).

3.1.4.Kinematic shear sense indicators

The sense of movement along the previously mentioned shear trends (E-W to ENE–WSW, N-S, NNW-SSE, NW-SE and WNW-ESE, NE-SW and NNE-SSW) can be detected by a wide variety of kinematic (shear sense) indicators. Kinematic indicators can be defined as structures developed at shear boundaries and within shear zones that are asymmetric with respect to both boundaries [29].

They can be developed at any scale from a single grain to tens of kilometers in diameter [30].In the concerned area, the kinematic indicators not only recognized at the outcrop-scale but also at the microscopic-scale. They include mylonite, boudinage structure and deformed pebbles.

Mylonite

Mylonite is a general term used to describe the deformed rocks that are exposed to plastic deformation and that leads to the grain size reduction. Mylonite is also recorded in El-Eridiya pluton associated with NE-SW shearing (Fig.12d).

Deformed pebbles

Deformed pebbles or deformed rocks are good indicators reflecting the sense of movement along the shear zone. The dextral sense of shear is recorded in El-Gidami pluton and associated with the NE-SW shearing (Fig.13a).

Porphyroclasts

Asymmetric porphyroclasts are common as σ –type. These structures are noticed in the amphibolitic rocks located at the northeastern part of Gabal Semna (Fig.13b).

3.2Tectonic evolution

The previous structural setting can be used to set up a comprehensive tectonic evolution of the study area in terms of the overall structural setting and tectonic evolution of both the ENS and ANS. The geological structures documented in the present study along the central QSSZ indicate an obvious brittle-ductile tectonic regime accompanied with voluminous granitic intrusions of various composition. The most striking structural feature in the study area is the presence of several intersected shear trends which can be arranged from oldest to youngest as follow: (1) E-W to ENE –WSW, (2) N-S, NNW-SSE, NW-SE and WNW- ESE, and (3) NE-SW and NNE-SSW. These trends are easily classified based on field work into strike-slip faults, shear zones and undefined shear fractures form widespread shear foliations deforming most of the outcropping granitic plutons, as well as the older structures in the ophiolitic mélange.

In places, the Najd-related (?) NW-SE sinistral faults/shear trends are transected by the E-W and study area in terms of the overall structural follow a youngest trend along the Egyptian Eastern Desert. SW dextral faults and shear zones, which can be regime accompanied with voluminous granitic intrusions of various composition. as follow: (1) setting and tectonic evolution of both the ENS and ANS. indicate an obvious brittle-ductile tectonic E-W to ENE –WSW, (2) N-S, NNW-SSE, NW-NE- interpreted as that the E- (to NE-) trending QSSZ The QSSZ follow a youngest trend along the Egyptian Eastern Desert. In addition, the documented shear trends and faults are associated with some related structures, like duplexex and flower structures which suggest right-lateral wrench-related tectonic activities along the QSSZ. Such structural and tectonic setting advocates a complex tectonic history characterized by interplay of extensional and transtensional tectonic regimes. The obtained results here support the results obtained by [30-31] concerning the structural and tectonic setting of the NED. In [29] the NED was referred to as an extensional province characterized by extensional faults and dyke swarms, and ascribed to the retreating of the Cadomian arc in Late Neoproterozoic-Cambrian time (Fig.13c). In [30] the fault striae analysis and paleostress reconstruction of the NED (using fault-slip data) suggested four paleostress tectonic regimes: transpression, transtension, transpression and extension (Fig.13d). These tectonic stages were related, respectively, to (1) the oblique convergence between E and W Gondwana, (2) the N to NNW-ward migration of the CED causing orogen-parallel extensional collapse to the NED, (3) the N–S shortening post-dating the formation of volcanosedimentary Hammamat Basins, and (4) the retreat of the Cadomian arc and the Red Sea rifting.

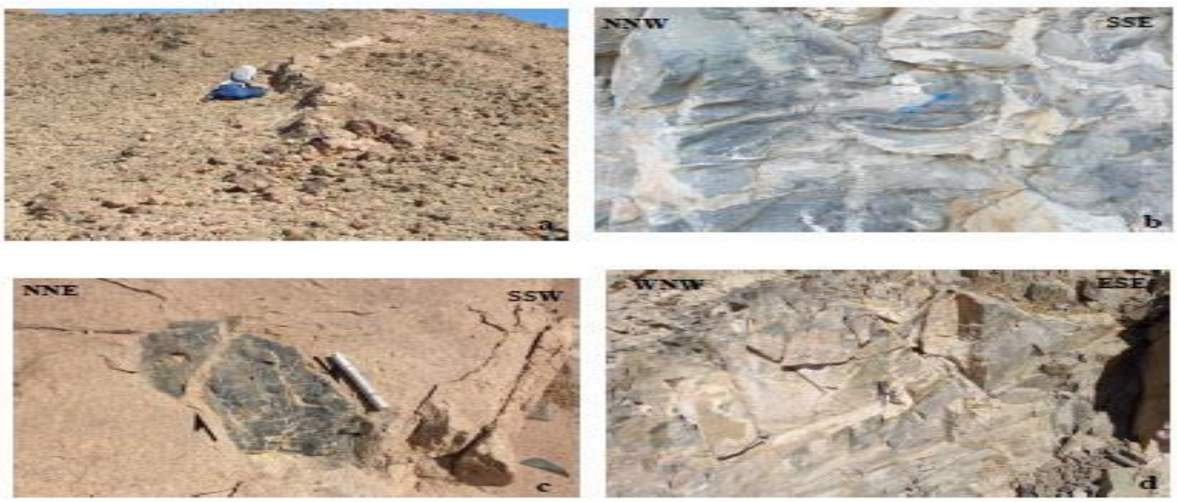

Fig(11) (a) Shear zone-related folding in El-Gidami syenogranites associated with the NE-SW shearing (b) Shear zone-related folding in the Dokhan Volcanics connected to the ENE -WSW shearing (c) Stretched amphibolite xenoliths in the tonalite rocks of Kafari pluton associated with the NNE shear trend (d) Mineral lineation defined by preferred orientation of mineral constituents in the quartz diorite rocks of El-Maghrabiya pluton

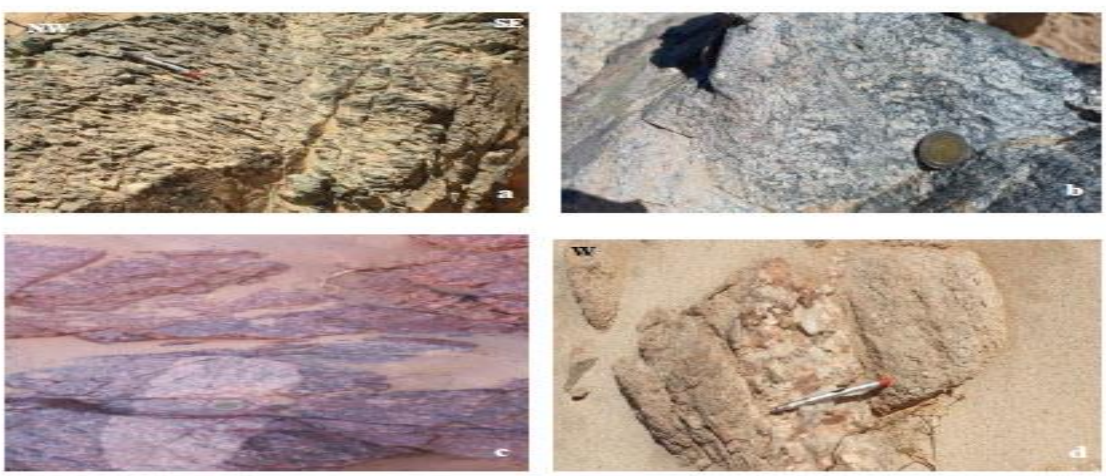

Fig(12) (a) Pencil lineation with moderate plunging in metaultramafic rocks located south to Kab Amiri pluton (b) General view of gneissose granite in the northern part of Rie El-Garra pluton showing gneissosity and quartz porphyroclasts (c) Mylonitized and pegmatitized syenogranites in El-Missikat pluton (d) Mylonitic zone recorded in El-Eridiya pluton associated with the NE–SW shearing.

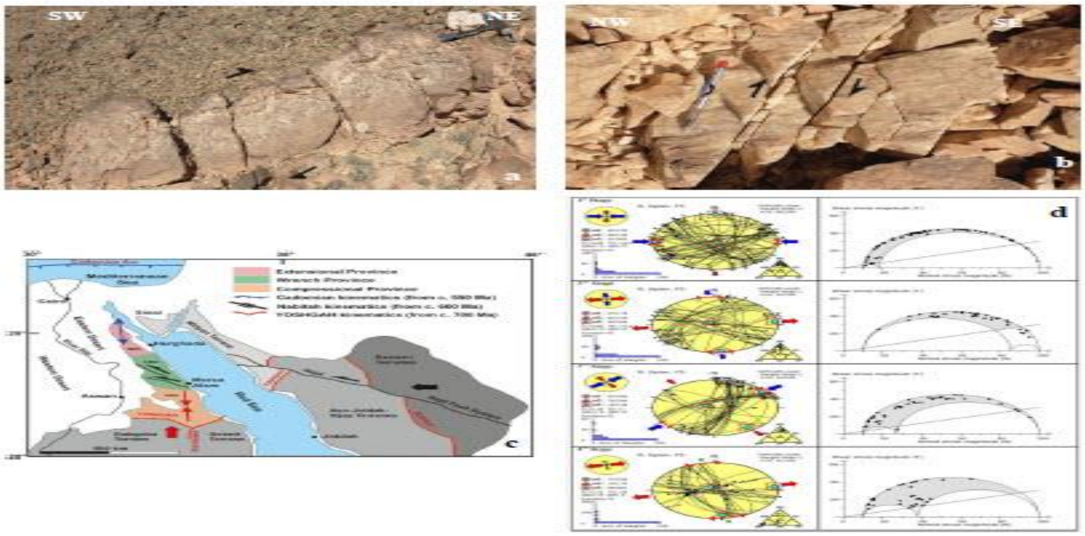

Fig(13)(a) Dextral sense of shearing in El-Gidami pluton associated with the NE-SW shearing trend (b) Dextral sense of shearing along the NE-SW shearing trend reflected by the monoclinic symmetry (σ- type) in Semna area (c) Plate tectonic situation and structural provinces related to different plate kinematics. The earliest event, convergence, and collision between Gabgaba-Gebeit terranes and the Eastern Desert terrane along the YOSHGAH suture released north-south compression (thick red arrow) and related north and south directed thrusts (red double arrow) in the southern compressional province. West—east convergence (thick black arrow) associated with Nabitah Orogeny caused modification of suture and W-E compression in the Hamisana Belt. In the northern portion, this motion is partitioned into large sinistral strike-slip systems of the Najd Fault System leading to transcurrent motion within the CED wrench province (black half arrows). The retreat of the northern Cadomian arc enabled extension in the northern NED extensional province (blue double arrow) [31], d) Stress stages obtained from the processing of fault data collected from areas I–VI in the NED [32].

4. Concluding remarks

1. The study area is covered by voluminous granitoids.
2. The oldest structures are highly obscured by the intrusion of granitoids.
3. Minor ophiolitic mélange is recorded in the study area and strongly deformed by shearing and intrusive rocks and dike swarms.
4. The main structural trends characterizing the area are E-W (to ENE-WSW) and NE-SW with minor and older NW-SE (to NNE-SSW).
5. Brittle- to brittle-ductile deformation highly controls the type and distribution of the geological structures,such as faults, lineations and shear zones along with the direct related structures like wrench related duplex and flower structures.
6. The structural grain of the study area suggests a transition from the wrench-induced transpressive structures along the CED (Najd-related deformation) to mostly extensional- (to transtensional-) related structures in the NED.

References

[1] S. El-Gaby, Architecture of the Egyptian basement com-plex. IBTA Association, Publ. (5), pp.1–8(1983).

[2] Z. Hamimi, M. A. El-Amawy and M. Wetait Geology and Structural Evolution of El-Shalul Dome and Environs, Central Eastern Desert, Egypt, Eg. J. Geol Vol. 38, pp. 575-595, 1994.

[3] M.L. El Rakaiby, The tectonic lineaments of the basement belt of the Eastern Desert, Egypt. EGJG, Vol. 32, p 77-95,1988.

[4] Y.A. El- kazzaz, Active faulting along Qena – safaga road, Eastern Desert, Egypt. The first international conference on the geology of Africa, Vol. 2,pp. 384-303, 1999.

[5] M.M. El Mansi, Coloration of fluorite and its relation to radioactivity. Egyptian Mineralogist, v.12,pp. 93-106,2000.

[6]M. K. Akaad, A. M. Noweir, Geology and lithostratigraphy of the Arabian Desert orogenic belt of Egypt between latitudes 24° 35̀ and 26° 30̀ N. IAG Vol.3, pp. 127-134, 1980.

[7] F.S. Bakhit and I.A. El Kassas, Distribution and orientation of radioactive veins in the El- Erediya El-Missikat area, Central Eastern Desert, Egypt. Egypt, Int. J. Remote Sens.Vol.10(3),pp. 464-481, 1989.

[8] N.A. Aly, H.A. Hegazy and A.A. El Tigrawy, Geology and petrochemistry of the arc volcanic in the Semna area, southwest of Safaga, Egypt. Sci. Bull.Assui. unvi.Vol. 20, pp.61–78, 1991.

[9]A. Abu Dief, S.E. Ammar and N.A. Mohamed, Geological and geochemical studies of black silica at El- Missikat pluton, Central Eastern Desert, Egypt. Proc. Egypt. Acad. Sci., Vol.37, pp.334-336, (1997).

[10] A.M. Moghazi, Petrology and geochemistry of Pan-African granitoids, Kab Amiri area, Egypt — implications of tectonomagmatic stages in the Nubian Shield evolution. Mineralogy and Petrology , Vol.74, pp.31–67, 2002.

[11] A.M. Dardier, Morphology, chemistry and Ucontents of biotite flakes of the older granitoids and younger granites, Gabal El-Maghrabiya area, Eastern Desert. DJS.Vol.28,pp.1-18, 2003.

[12]F.S. Bakhit, H.A. Hussein, and M.M. Ali, Geotectonics and characteristics features of fertile and non-fertile younger granites , Eastern Desert, Egypt. Basement Tectonics, Vol.13,pp.1-23, 2007.

[13] B. Zoheir, A. Akawy and I. HassanRole of fluid mixing and wallrock sulfidation in gold mineralization at the Semna mine area, central Eastern Desert of Egypt: Evidence from hydrothermal alteration, fluid inclusions and stable isotope data. Ore Geol. Rev., Vol. 33, pp. 480–496, 2008.

[14]A. Abdel warith, M., Michalik and B.H. Ali Luorine enriched granites: chemical characterization and relation to uranium mineralization. Journal of Applied Sciences Research, Vol.6, pp.299- 323,2010.

[15] A. Asran and E. Abdel Rahman, The Pan-African calc-alkaline granitoids and the associated mafic microgranular enclaves (MME) around Wadi Abu Zawal area, North Eastern Desert, Egypt: geology, geochemistry and petrogenesis. J. Biol. Earth Sci.Vol.2,pp.1-16, 2012..

[16] H.A. Eliwa, J.I. Kimura and T. Itaya , Late Neoproterozoic Dokhan Volcanics, north Eastern Desert, Egypt: Geochemistry and petrogenesis . Precambrian Res., Vol. 141, pp.31-42, 2006.

[17]Sh. Kharbish, and A. El- Awady, Geochemistry and geotectonic significance of Neoproterozoic ophiolitic prediotites and pyroxenites, kab Amiri, Eastern Desert, Egypt. J. Environ. Manag. , v.xx, pp. 38-34, 2018.

[18]H. El Sundoly impact of tectonic factors on the emplacement of the radioactive mineralized pegmatites of Wadi Abu Zawal area, North Eastern Desert, Egypt. Curr. Sci. Int.,Vol.10,pp178-199, 2021..

[19] L.Q. Hung, Remote sensing based hydrogeological analysis of Suoimuoi catchment Vietnam. M.Sc., Thesis, VUB, 87p, 2001.

[20]L.Q. Hung, and O. Batelaan, Environmental geological remote sensing and GIS analysis of tropical karst areas in Vietnam. IGARSS, Vol. 3, pp. 2963-2966, 2003.

[21]G.B. Kim, J.Y. Lee and K. K. Lee, Construction of lineament maps related to groundwater occurrence with ArcView and Avenue TM scripts. Comput and Geosci Vol. 30, pp. 1117–1126,2003..

[22] M.J. Smith, and C. D. Clark, Methods for the visualization of digital elevation models for landform mapping. Earth Surface Processes and landforms, Vol.30(7), pp.884–900, 2004.

[23] S. M. El-Hebiry, Geological setting and structural pattern of the basement rocks of Wadi Um Gheig Area, central Eastern Desert in light of the field studies and Remote Sensing interpretation. M .Sc., Thesis, AZU Cairo, 177p, 2013.

[24] L. Han, Z. Liu, Y. Ning and Z. Zhao, Extraction and analysis of geologic al lineaments combining a DEM and remote sensing images from the northern Baoji loess Area. ASR, Vol. 62(9), pp. 2380-2393, 2018.

[25]A, Madani, Knowledge-driven GIS modeling technique for gold exploration, Bulghah gold mine area, Saudi Arabia. Egypt. J. Remote Sens. Space Sci.Vol.14,pp.91-97, (2011).

[26] E. Crepani and J.S. Medeiros, Imagens fotográficas derivadas de MNT do Projeto SRTM para fotointerpretação na Geologia, Geomorfologia e Pedologia.Crepani; J. S. de Medeiros. São José dos Campos: INPE, 1993.

[27] B. A. Van der Pluijm and S. Marshak, Earth structure: an introduction to structural geology and tectonics. W.W. Norton and Company, 646pp, 2003..

[28]H. Fossen, Structural Geology. 2nd Ed., Printed in the United Kingdom by clays, St Ives plc, 510p, 2016.

[29] C. Passchier, and C. Simpson. Porophyroclast systems as kinematic indicators: J. Struct. Geol., Vol. 8, p. 831-833,1986..

[30]J. J. Jr. Gallagher, Tectonics of China: Continental scale cataclastic flow; pp. 249-273 in N. L. Carter, M. Friedman, J. M. Logan, and D. W. Stearns (eds.), Mechanical Behavior of Crustal Rocks: American Geophysical Union, Geophysical Monograph , Vol.23,326 p, 1981.

[31] Z. Hamimi, W. Hagag, H. Fritz, H. Baggazi and S.Z. Kamh The Tectonic Map and Structural Provinces of the Late Neoproterozoic Egyptian Nubian Shield: Implications for Crustal Growth of the Arabian–Nubian Shield (East African Orogen), Front. Earth Sci.Vo.10, 2022.

[32] Z. Hamimi, A.M. Eldosouky, W. Hagag and,S.Z Kamh, Large-scale geological structures of the Egyptian Nubian Shield. Scientific Reports, 2023.